

NOVEL CERIA AND CERIA-BASED NANOCOMPOSITES
AS POTENTIAL CATALYSTS FOR METHANOL
DECOMPOSITION AND TOTAL OXIDATION OF ETHYL
ACETATE

Momtchil Dimitrov, Gloria Issa[#], Daniela Kovacheva*,
Tanya Tsoncheva

Received on November 22, 2021

Presented by Ch. Tsvetanov, Member of BAS, on June 21, 2022

Abstract

The focus of our study is the development of novel ceria-based materials that can be successfully used as catalysts in various environmentally friendly processes due to a significant improvement of ceria intrinsic characteristics. In particular, the combination of ceria with low-dimensional carbon materials such as graphene oxide (GO) and nanodiamond (ND) appears as a very promising approach. Actually, the decrease of ceria crystallite sizes deep in the nanoscale have been found to convert them into highly effective destructive adsorbent materials owing to their high surface area, strong adsorbability, and large number of highly reactive sites. Besides, the addition of a nanostructured carbon containing component (nanodiamond or graphene oxide) contributes to both mechanical and catalytic properties of the obtained nanocomposite hybrids. The results show that the novel ceria and ceria-based composite materials significantly outperform the hydrothermally obtained ceria catalyst used for comparison in both activity and selectivity to CO and hydrogen in the methanol decomposition reaction, and in the process of total oxidation of ethyl acetate due to their significantly improved redox behaviour and textural characteristics.

[#]Corresponding author.

Financial support from project KP-06-PM-39/1/2019 is acknowledged. The bilateral project IC-CZ/04/2020-2022 between BAS and Czech Academy of Sciences for scientific support is also acknowledged.

DOI:10.7546/CRABS.2022.09.05

Key words: nanosized ceria, ceria-nanodiamond and ceria-graphene oxide nanocomposite hybrids

Introduction. Ceria is one of the most used metal oxides in various catalytic applications due to its intrinsic redox ability [1]. If the size of its building crystallites decreases deep in the nanometer scale, an increase in their specific reactivity is expected to be registered [2]. Such acceleration of the reactions that occur on the surface of ceria nanocrystals could be attributed to several factors. One of them is the increase in the number of edges, corners and dislocations, which would lead to the presence of higher amount of cerium cations with low coordination number, which favours their reactivity [3]. Another factor is the diffusion of reactants to and fro to these active sites, and the presence of very small ceria crystallites could significantly facilitate this process as such a system will be characterized by higher specific surface area and more importantly a great part of it will be due to the more readily accessible and bigger in proportion outer surface in comparison with analogous materials comprised of bulkier ceria crystallites.

At the same time, the combination of nanostructured metal oxide with carbon materials (nanodiamond or graphene oxide) would lead to the formation of a nanocomposite hybrid material with improved textural and chemical functionality [4-6]. Besides the expected increase in the specific surface area of the hybrid materials, the presence of oxygen-containing groups within the carbon component would ensure good bonding and interfacial interactions with the metal oxide component that would prevent agglomeration processes and could lead to the occurrence of synergistic effects, and hence to the appearance of new properties that differ from those of the individual components. However, the fine control of the size and distribution of the ceria nanomaterial on graphene oxide or nanodiamond is still a major challenge to the development of carbon-containing ceria hybrids for widespread applications, and little research has been focused on the use of the different synthetic strategies [7,8].

In this study we investigate the role of the addition of two different carbon components (nanodiamond and graphene oxide) to the synthesis solution for the preparation of nanosized ceria hybrid nanocomposite materials that will be tested as catalysts for two environmentally friendly reactions, namely total oxidation of ethyl acetate as a representative of volatile organic compounds (VOCs) and methanol decomposition to hydrogen and CO as an alternative fuel source. By using a combination of various characterization techniques as X-ray diffraction, nitrogen physisorption, Raman- and UV-Vis spectroscopy, and temperature-programmed reduction with hydrogen we would be able to elucidate some important characteristics and properties of the obtained novel ceria-based nanomaterials.

Experimental. Materials. The novel ceria and ceria-based nanocomposite hybrid materials were synthesized at room temperature. In a typical synthesis, 500

mL of 20 mM cerium(III) nitrate solution mixed with desired amount of Graphene Oxide (GO) (0; 10 wt.%) or (ND) (0; 10 wt.%) in a closed stirred beaker was purged by CO₂-free air (CO₂ was removed by passing through 1 M KOH solution to prevent undesired formation of carbonates) for a couple of minutes and heated to 303 K. The slow addition of 20 mL ammonia solution to adjust pH above 10 led to precipitation cerium hydroxide. The mixture was further stirred and purged with CO₂-free air until it transformed to CeO₂. The obtained powder was washed with deionized water several times and dried. GO composite samples were dried by lyophilization with liquid nitrogen. ND composite samples were air-dried at 333 K. The samples were denoted as Ce-GOL_xx, where “xx” is the percentage by weight amount of GO and Ce-ND_yy, where “yy” is the percentage by weight amount of ND. For comparison was prepared a reference ceria sample, designated CeO₂-HT, by using a template-assisted precipitation approach in combination with hydrothermal treatment at 373 K for 24 h followed by a calcination step at 773 K for 10 h [9].

Methods of investigation. Powder X-ray diffraction (XRD) study was performed on a Bruker D8 Advance diffractometer (Bruker AXS GmbH, Germany) with Cu K α radiation and a LynxEye detector with constant step of 0.02° 2 θ and counting time of 17.5 s per step. The mean crystallite sizes were determined by the Topas-4.2 software. The texture of the pure ceria samples and the ceria-based nanocomposite hybrids was studied by low-temperature nitrogen physisorption in a Quantachrome Instruments NOVA 1200e (USA) apparatus. The specific surface area was determined from Brunauer–Emmett–Teller (BET) equation, the total pore volume was obtained at a relative pressure of 0.99, and Barrett–Joyner–Halenda method was used for the analysis of the pore size distribution. The Raman spectra were acquired with a DXR Raman microscope (Thermo Fischer Scientific, Inc., Waltham, MA) using a 780 nm laser. The UV-Vis spectra were recorded on a Jasco V-650 UV-Vis spectrophotometer equipped with a diffuse reflectance unit. The Thermo-Gravimetric-Temperature Programmed Reduction (TG-TPR) study was performed on a Setaram TG 92 instrument (SETARAM Instrumentation, France) in a mixture of hydrogen and argon (100 cm³.min⁻¹, volume ratio of H₂ : Ar = 1) and heating rate of 5 K.min⁻¹.

Catalytic tests. The methanol decomposition catalytic tests were carried out in a flow type fixed bed reactor with methanol partial pressure of 1.57 kPa, Ar being used as a carrier gas. The catalysts were tested under a temperature-programmed regime within the range of 350–770 K with a heating rate of 1 K.min⁻¹. On-line gas chromatographic analyses were performed on a HP 5890 apparatus equipped with flame ionization and thermo-conductivity detectors, on a PLOT Q column. Absolute calibration method and a carbon-based material balance were used for the calculation of methanol conversion and the products yields.

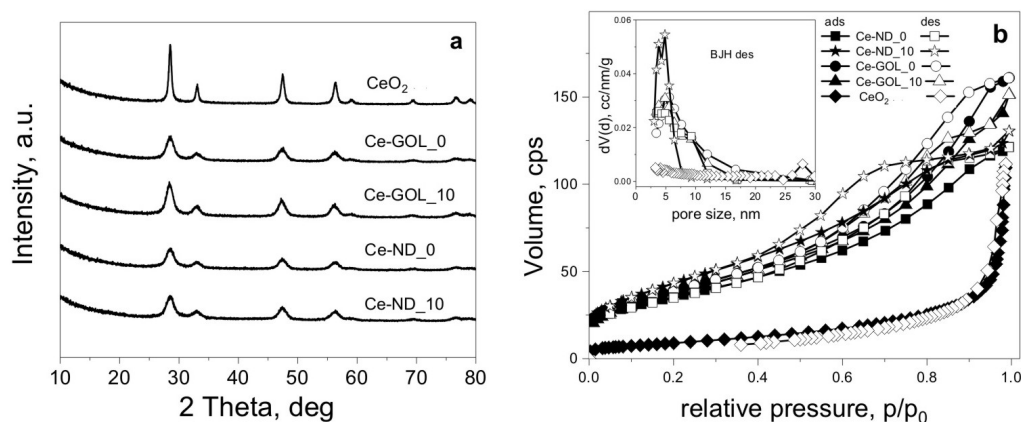


Fig. 1. XRD patterns (a) and data from nitrogen physisorption analysis (b)

Ethyl acetate total oxidation experiments were performed in a flow type reactor with a mixture of ethyl acetate in air and WHSV of 100 h^{-1} . Gas chromatographic analyses were done on a HP 5890 apparatus using carbon-based calibration.

Results and discussion. In order to get information for the phase composition of the synthesized samples powder X-ray diffraction technique was used. The obtained X-ray diffraction patterns reveal the presence of face-centred cubic cerianite phase in all studied samples (Fig. 1a, Table 1). In case of novel ceria and ceria-based nanocomposite samples, the obtained reflections are broader and the calculated size of the ceria crystallites is about 7 nm. It seems that the addition of carbon-containing phase (nanodiamond or graphene oxide) does not influence the size of the obtained ceria crystallites. At the same time, the reference CeO_2 -HT sample is comprised of bigger ceria crystallites with sizes of about 18 nm. The found significant difference we ascribe to the novel synthetic procedure where the synthesis of ceria phase occurs at 303 K.

For the elucidation of the textural differences in the studied samples a nitrogen physisorption analysis was performed. The results show that all novel ceria samples are mesoporous with pore sizes within a relatively narrow range of 3–15 nm, their isotherms are of type IV according to IUPAC classification, characterized by H1 hysteresis due to the presence of cylindrical pores, which could favour the mass transport through these materials (Fig. 1b, Table 1). Besides, the registered high values for the specific surface area and total pore volume make them potentially very attractive for use as adsorbents or catalysts. It seems that the addition of graphene oxide practically does not change the textural characteristics of the obtained nanocomposite, while the addition of nanodiamond even has its contribution in getting the highest specific surface area among the studied samples. On the other hand, the reference ceria sample is characterized by much

broader pore size distribution with the predominant presence of less in number larger mesopores (Fig. 1b, Table 1). Moreover, a much lower specific surface area and lower total pore volume were found for CeO₂-HT, which we ascribe to its much more compact texture.

Table 1

Powder X-ray diffraction and nitrogen physisorption data for the pure nanosized ceria samples and the ceria-based nanocomposite hybrids

Sample	Phase composition	Cell parameters, Å	Crystallite size, nm	S _{BET} , m ² ·g ⁻¹	V _{total} , cm ³ ·g ⁻¹
Ce-GOL_0	CeO ₂ , Cubic Fm-3m	5.423 (1)	7	141	0.25
Ce-GOL_10	CeO ₂ , Cubic Fm-3m	5.422 (1)	7	137	0.23
Ce-ND_0	CeO ₂ , Cubic Fm-3m	5.421 (2)	7	127	0.19
Ce-ND_10	CeO ₂ , Cubic Fm-3m	5.421 (1)	7	160	0.20
CeO ₂ -HT	CeO ₂ , Cubic Fm-3m	5.4147(4)	18	33	0.14

For elucidation of some structural peculiarities of the studied materials Raman and UV-Vis analysis were performed (not shown). In the Raman spectra of all novel ceria and ceria hybrid materials, a slight broadening together with a decrease in the intensity and a slight shift to lower values (about 454 cm⁻¹) of the main characteristic band of ceria is registered in comparison with the reference CeO₂-HT sample (461 cm⁻¹). The observed differences could be ascribed to both the presence of ceria crystallites in very highly dispersed state and to

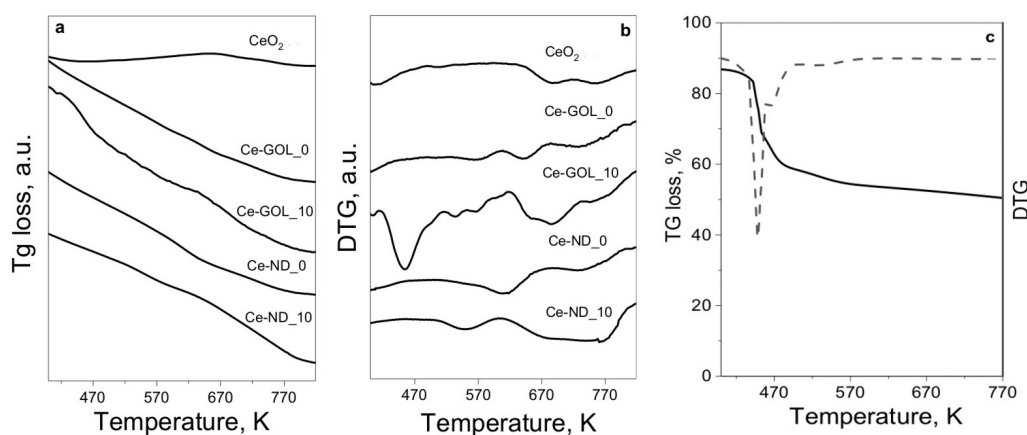


Fig. 2. TPR-TG (a) and TPR-DTG (b) profiles for the studied samples, and TPR data for the pure graphene oxide material (c)

their interaction with either the nanodiamond or graphene oxide additive. The UV-Vis spectra reveal an increase in the absorption ability of Ce-ND_10 and Ce-GOL_10 samples in the visible range. It seems that the presence of carbon phase seems to facilitate the charge transfer in the visible range, and the latter is more pronounced for the Ce-GOL_10 nanocomposite hybrid.

The redox properties of the obtained modifications are characterized under the conditions of temperature-programmed reduction with hydrogen (Fig. 2). The TPR-TG profiles of all novel ceria samples show an almost constant weight loss in the 400–773 K range (Fig. 2a). We could ascribe the observed effect to surface reduction of Ce^{4+} to Ce^{3+} of the very small ceria crystallites, as their outer surface is much bigger and readily accessible. Besides, the presence of oxygen-containing groups in the ceria nanocomposite hybrids also contributes to this feature, especially in case of Ce-GOL_10 sample where the registered weight loss in the low temperature range of 450–600 K was significant and due to the release of oxygen-containing functionalities from the graphene oxide (Fig. 2c). At the same time, the reference CeO_2 -HT samples show only a slight weight loss above 620 K due to surface reduction of its bigger ceria particles.

Catalytic tests. Methanol decomposition was performed in a temperature-programmed regime within the range of 350–770 K (Fig. 3a, b). The novel ceria materials start to decompose methanol at about 600 K and show a steep increase in their activity above 650–700 K reaching between 65 and 95% conversion ability. Moreover, their selectivity to CO and, respectively, to hydrogen production is quite high and stable (about 60–70%) at high conversion rates. It should be noted that the addition of both nanodiamond and graphene oxide improves the catalytic activity, and we could ascribe that to the appearance of synergistic effect within the nanocomposite hybrids. At the same time, the reference CeO_2 -HT sample starts to decompose methanol just above 700 K and shows a maximum conversion ability of about 50% in combination with a very low selectivity to CO (Fig. 3a, b).

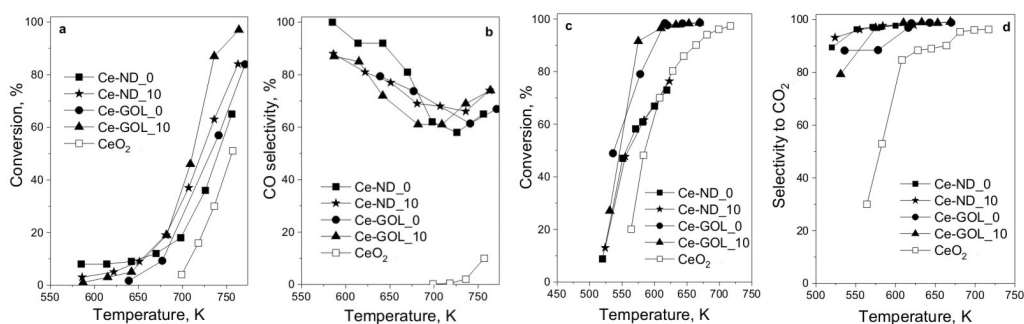


Fig. 3. Temperature dependencies of methanol decomposition: (a) activity and (b) selectivity to CO (b) and temperature dependencies of ethyl acetate oxidation: (c) activity and (d) selectivity to CO_2 on the studied samples

The observed differences in the catalytic behaviour of the novel ceria materials and the reference ceria sample we ascribe to both the much bigger and highly reactive surface of the novel ceria and ceria nanocomposite hybrid materials that could readily adsorb methanol molecule at lower temperatures and to their significantly improved redox properties.

Ethyl acetate total conversion was performed within 450–700 K temperature range, (Fig. 3c, d). All novel ceria materials show higher catalytic activity than the reference CeO₂-HT sample, especially at low temperatures. Among the ceria nanocomposites the Ce-GOL_10 sample shows significantly higher activity with above 90% conversion ability at about 570 K (Fig. 3c). Usually, the ethyl acetate oxidation is a step-wise process, including first a hydrolysis to ethanol and acetic acid followed by their oxidation via Mars–Van Krevelen mechanism. Hence, we could expect a higher amount of by-products at low conversion rates. And this is the case with the reference ceria sample (Fig. 3d). However, in the case of the novel ceria materials, the selectivity to total oxidation is very high (above 80%) even right from the start of the ethyl acetate conversion (Fig. 3d). It seems that almost immediately the formed by-products from ethyl acetate hydrolysis are being oxidized and we ascribe that to the significantly improved redox properties of the novel ceria materials.

Conclusions. The novel ceria-based nanocomposites are comprised of very small ceria nanocrystallites and possess small and homogeneous mesopores that give rise to high specific surface areas and total pore volumes. The complex physicochemical characterization of the obtained nanocomposites reveals that they are more reactive and able to release oxygen under reductive medium in comparison with the reference hydrothermally treated ceria sample. The presence of carbon phase, especially graphene oxide, seems to facilitate the charge transfer in the visible range. The catalytic results show that the novel ceria and ceria-based composite materials significantly outperform the reference ceria catalyst in both activity and selectivity to CO and hydrogen in the methanol decomposition reaction, and in the activity and selectivity to total oxidation of ethyl acetate. We assign these results to the significantly improved redox behaviour and textural characteristics of the synthesized novel ceria nanocomposite materials. Further investigations of these new nanocomposite ceria-based hybrid systems as supports for other metal/metal oxides are in progress.

Acknowledgements. The authors thank Jakub Tolasz from Institute of Inorganic Chemistry of the Czech Academy of Sciences for synthesis of the novel ceria-based samples.

REFERENCES

- [¹] TROVARELLI A. (1996) Catalytic properties of ceria and CeO₂-containing materials, *Catal. Rev.*, **38**, 439–520.
- [²] WANG D., T. XIE, Y. LI (2009) Nanocrystals: Solution-based synthesis and applications as nanocatalysts, *Nano Res.*, **2**, 30–46.
- [³] SAYLE D. C., S. SEAL, Z. WANG, B. C. MANGILI, D. W. PRICE et al. (2008) Mapping nanostructure: a systematic enumeration of nanomaterials by assembling nanobuilding blocks at crystallographic positions, *ACS Nano*, **2**(6), 1237–1251.
- [⁴] KIM H. I., H.-N. KIM, S. WEON, G.-H. MOON, J.-H. KIM et al. (2016) Robust co-catalytic performance of nanodiamonds loaded on WO₃ for the decomposition of volatile organic compounds under visible light, *ACS Catal.*, **6**, 8350–8360.
- [⁵] LI X., R. SHEN, S. MA, X. CHEN, J. XIE (2018) Graphene-based heterojunction photo-catalysts, *Appl. Surf. Sci.*, **430**, 53–107.
- [⁶] MORALES-TORRES S., L. M. PASTRANA-MARTÍNEZ, J. L. FIGUEIREDO, J. L. FARIA, A. M. T. SILVA (2013) Graphene oxide-P25 photocatalysts for degradation of diphenhydramine pharmaceutical and methyl orange dye, *Appl. Surf. Sci.*, **275**, 361–368.
- [⁷] MIN C., Z. HE, H. SONG, D. LIU, W. JIA et al. (2019) Fabrication of Novel CeO₂/GO/CNTs Ternary Nanocomposites with Enhanced Tribological Performance, *Appl. Sci.*, **9**, 170.
- [⁸] BAI G., J. WANG, Z. YANG, H. WANG, Z. WANG et al. (2014) Preparation of a highly effective lubricating oil additive – ceria/graphene composite, *RSC Adv.*, **4**, 47096–47105.
- [⁹] IVANOVA R. N., M. D. DIMITROV, G. S. ISSA, D. G. KOVACHEVA, T. S. TSONCHEVA (2018) Catalytic oxidation of ethyl acetate by copper modified Ce-Mn and Ce-Ti mesoporous nanostructured oxides, *Bulg. Chem. Commun.*, **50**, 179–185.

*Institute of Organic Chemistry
with Centre of Phytochemistry
Bulgarian Academy of Sciences
Akad. G. Bonchev St, Bl. 9
1113 Sofia, Bulgaria*

e-mail: gloria.issa@orgchm.bas.bg
momtchil.dimitrov@orgchm.bas.bg
Tanya.Tsoncheva@orgchm.bas.bg

**Institute of General
and Inorganic Chemistry
Bulgarian Academy of Sciences
Akad. G. Bonchev St, Bl. 11
1113 Sofia, Bulgaria*

e-mail: didka@svr.igic.bas.bg